Relaxation of radiation damage in silicon planar detectors

B. Schmidt
Forschungszentrum Rossendorf, P.O. Box 51 01 19, D-01314 Dresden, Germany

V. Eremin, A. Ivanov, N. Strokan, and E. Verbitskaya
Ioffe Physico-Technical Institute, Russian Academy of Sciences, SU-194021 St. Petersburg, Russia, CIS

Z. Li
Brookhaven National Laboratory, Upton, New York 11973

(Received 31 March 1994; accepted for publication 27 June 1994)

The behavior of radiation-induced carbon-related defects in high-resistivity silicon detectors has been investigated. The defects were introduced by α-particle irradiation and investigated by deep-level transient spectroscopy. An unusual defect behavior consists in low-temperature annealing, including self-annealing at room temperature, of the interstitial carbon C_i with a simultaneous increase of the C_i-O_i-complex concentration. The kinetic parameters of the process have been determined from the increase of the C_i-center concentration versus time. Two annealing velocities have been observed, which arise from different heat treatments during the detector fabrication process.

I. INTRODUCTION

Relatively stable radiation defect structures such as vacancy-impurity pairs, interstitial-impurity atom pairs, and multiple-vacancy "clusters" are known which produce electronic states characterized by specific energy levels in the band gap. The changes in the electronic properties of silicon detectors are interpreted by these defect levels which are often deep levels. Deep defect levels act as charge carrier traps, which critically affect the current-voltage (I-V) and capacitance-voltage (C-V) characteristics and which can reduce the charge collection efficiency (energy resolution of the detector), the carrier mobility, or can change the majority-carrier concentration and affect the apparent bulk material resistivity.[1–3] Thus, a large effort is devoted to minimize the radiation-induced detector degradation and to develop technologies for radiation-hardened silicon detectors for the application of silicon detectors in high-energy physics.

The radiation-induced degradation of semiconductor detectors has been investigated intensively during the past years using mostly high-energy electrons, neutrons, or protons as incident particles. Nevertheless, the physical interpretation of radiation-induced defect generation and its influence on the detector characteristics is not yet clear for many observed radiation effects. One of these effects is the partial recovery of the radiation-degraded reverse current of the detectors at room temperature, the so-called "self-annealing" effect.[4–7] From these investigations it can be concluded that the self-annealing effect is based on the reformation of radiation defects. Therefore, a change in the spectrum of deep levels in the band gap of silicon can be observed.

The behavior of the most active impurities in the interaction with radiation-induced primary defects in n-type silicon is well known. Such impurities are phosphorous as well as oxygen and carbon. Phosphorous and oxygen atoms interact with vacancies and form P-V and O-V centers, the so-called E and A centers, respectively. The behavior and the characteristic parameters of these centers have been studied in detail. Concerning carbon-related radiation defects in n-type float-zone silicon (FZ Si), increasing interest is focused especially on the properties of the long-time instability of these defects.[7–11] A metastability can be observed, which means that an increase or decrease of the concentration of free charge carriers in the space-charge region can drastically change the defect energy levels in the band gap.

Most investigations of carbon-related defects have been done on low-resistivity Czochralski silicon (Cz Si) with $\rho \leqslant 10\ \Omega$ cm. The results of these studies cannot be transfered without additional investigations to the detector-grade silicon, because this material is high-purity FZ Si, usually n-type (phosphorous doped) with a resistivity of $\rho \geqslant 1000\ \Omega$ cm and low concentration of other impurities in the crystal. The process of crystal growth has a decisive influence especially on the carbon and oxygen content. Usually the C and O concentrations in FZ Si are lower by approximately one order of magnitude than in Cz Si.

The aim of this article is to investigate the time behavior of α-particle-induced carbon-related defects in high-resistivity n-type FZ silicon. In addition, the behavior of silicon material from different manufacturers as well as the effect of variations in the fabrication technology of the detector on the defect properties are studied.

II. EXPERIMENTAL PROCEDURE

The samples used in the present investigations were p-n junction detectors with a p^+-n-n^+ structure made from n-type FZ Si with a resistivity of $\rho = 1$–$2\ \mathrm{k}\Omega$ cm (Freiberger Elektronikwerkstoffe GmbH) and of $\rho = 5\ \mathrm{k}\Omega$ cm (Wacker Chemitronic Burkhausen). The detectors are ion-implanted planar diodes with an active area of $A = 25\ \mathrm{mm}^2$ and a thickness of 300 μm. The p^+ and n^+ layers were fabricated using ion implantation of boron and phosphorous, respectively. The postimplantation annealing was carried out in an inert gas atmosphere. The detector surface was passivated by thermally grown SiO_2 with various layer thicknesses from 1000 up to 9000 Å.

 0021-8979/94/76(7)/4072/5/$6.00

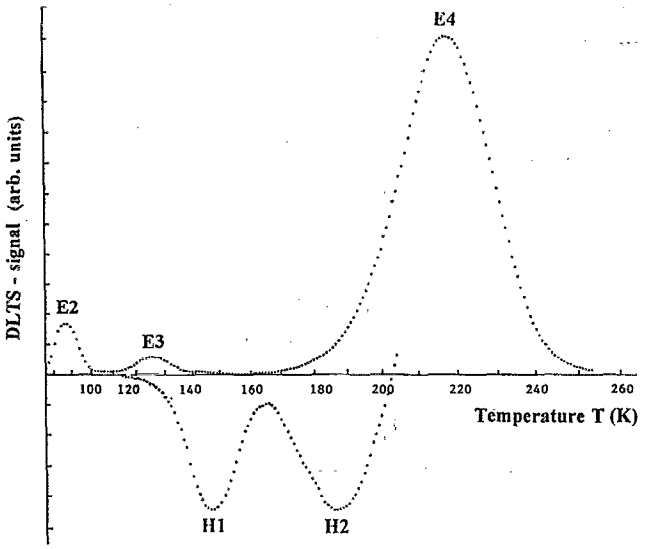

FIG. 1. DLTS spectra of α-particle-irradiated silicon detectors.

Radiation defects have been introduced into the detector structure, cooled to $T \simeq 200$ K, by irradiation through the p^+ layer using α particles from a ^{238}Pu source with a particle energy of $E_\alpha = 5.487$ MeV. The irradiation dose was $D_\alpha = 1 \times 10^9$ cm^{-2} and the mean range of the α particles in silicon was about 25 μm.

The spectra of α-particle-induced defects were measured using deep-level transient spectroscopy (DLTS). The DLTS analysis has been performed at a frequency of 100 kHz and with a rate window of 41.7 ms. The amplitude of the reverse-bias-voltage pulse was chosen as $U_{r,\text{pulse}} = 5$ V. The corresponding depletion layer width of $w = 35$–90 μm exceeds the layer depth, where the defects arise during α-particle irradiation. Obviously, under these conditions the properties of the detector bulk silicon will be preserved during later annealing of the radiation-induced defects. It should be mentioned that at low irradiation doses of $D_\alpha = 1 \times 10^9$ cm^{-2} we can exclude any disturbance (e.g., peak broadening and shifting) of the DLTS spectra, which is usually observed in high-dose irradiated ($D_\alpha \geq 10^{10}$ cm^{-2}) silicon diodes, and hampers the interpretation of experimental results.

III. EXPERIMENTAL RESULTS

A. Isothermal low-temperature annealing

Figure 1 shows the DLTS spectrum of defects generated in the detector samples during α-particle irradiation. Table I summarizes the parameters of the levels observed in the DLTS spectrum, together with information from the literature.

It should be mentioned that most of the published data are related to experiments in which electron irradiation of silicon has been carried out.[11,12] Nevertheless, these results can be used for the interpretation of the α-particle-induced defects.[5]

As shown in Fig. 1, the DLTS spectrum contains three energy levels of carbon-related defects,[5,10,11] but only the two peaks H1 and H2 in the lower half of the band gap have been investigated in this article more in detail. The choice of these two levels was determined by the following circumstances.

TABLE I. Parameters of deep levels in silicon after irradiation.

Level type	Level energy (eV)	Capture cross sections σ_n and σ_p[a] ($\times 10^{-14}$ cm^2)	References
E1	$E_c - 0.12$	...	10 and 11
E2	$E_c - 0.18$	2	This work
E3	$E_c - 0.22$	0.02	and
E4	$E_c - 0.40$	0.02	Ref. 5
H1	$E_v - 0.33$	9	
H2	$E_v - 0.40$	3	

[a]In the case of H1 and H2 the cross sections are labeled by σ_p and for the other levels by σ_n.

First, the Fermi level of high-resistivity silicon is localized at a lower position than the carbon-related defects E1 (Ref. 11) and E2 observed in this work, which are located in the upper half of the band gap. Therefore, we can assume that the charge carrier filling factor of the centers during the voltage pulse $U_f \simeq 0$ V is quite small, but it can change during the defect annealing and it will be difficult to get quantitative information from the measurements. Furthermore, as pointed out in Ref. 11 the H1 center represents the interstitial carbon in the donor state and the E1 center is the interstitial carbon in the acceptor state. Therefore, the data of the investigated H1 concentration are also valid for the E1 center.

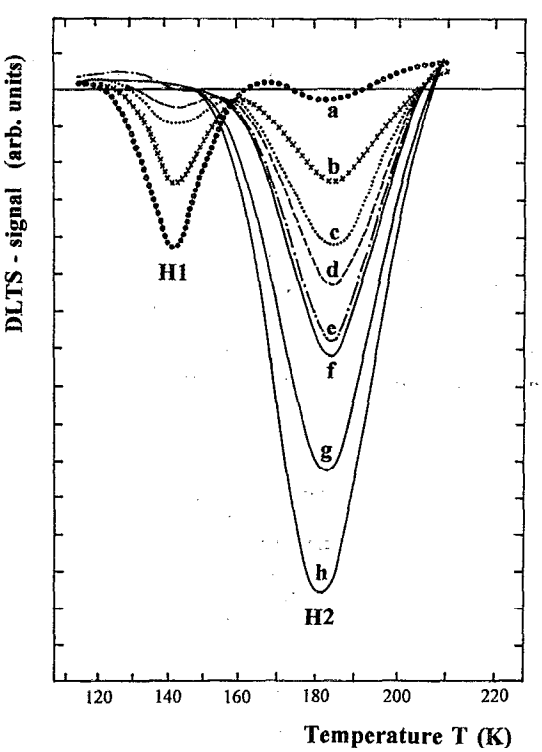

FIG. 2. Change of the DLTS spectra vs annealing time at room temperature (sample no. BNL 213): (a) immediately after irradiation, (b) 2 h, (c) 5.5 h, (d) 8.5 h, (e) 15 h, (f) 17.5 h, (g) 41.5 h, (h) 217.5 h.

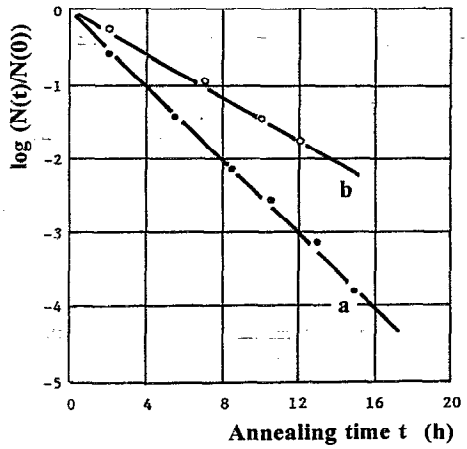

FIG. 3. Concentration decrease of the H1 center vs annealing time: (a) $T=19$ °C, fast sample no. BNL 213; (b) $T=50$ °C, slow sample no. FZR 2-1.

Second, the more shallow centers E1 and E2 (relative to H1 and H2) have a small influence on the generation current, one of the most important quality parameters of semiconductor detectors.

Figure 2 depicts the typical concentration changes of the H1 and H2 centers versus time at room temperature after α-particle irradiation. It can be seen that during annealing of the H1 center the concentration of the H2 center increases. The conditions of constant hole filling of the H1 and H2 centers, located below the Fermi level, enable the relative concentration changes to be measured.

As seen from Fig. 3 an exponential concentration decrease of the H1 center has been observed. This behavior can be described using the equation of a first-order reaction,

$$N^1(t)=N_0^1 \exp\left(-\frac{t}{\tau}\right), \tag{1}$$

where N_0^1 is the starting concentration of the H1 center and τ is the mean lifetime of the center. Furthermore, the annealing rate of the H1 center is quite different for detectors prepared in high-resistivity silicon from two different manufacturers (see Table II), although the defect generation in the two silicon materials is quite similar. The concentration N_0^1 for the H1 center amounts to 9.4×10^{10} and 2.4×10^{11} cm^{-3} for silicon from Wacker Chemitronic and Freiberger Elektronikwerkstoffe, respectively.

B. Temperature dependence of the annealing rate

We have further determined the excitation energy for the relaxation of the H1 center near room temperature. We conclude that this relaxation is determined by the diffusion of interstitial carbon in the silicon crystal. Thereby the interstitial carbon C_i may be captured by the interstitial oxygen O_i to form the C_i-O_i center or by the substitutional carbon C_s to form the complex C_s-C_i.[8] This C_i diffusion process can be described by the effective migration energy of carbon ΔE_m, which can be determined from the temperature dependence of the annealing rate according to

$$\frac{1}{\tau}=A \exp\left(\frac{-\Delta E_m}{kT}\right), \tag{2}$$

where τ denotes the mean lifetime, k the Boltzmann constant, and A a constant parameter.

Table II shows that the values of ΔE_m are significantly different for the two investigated detectors. It should be pointed out that the lower value $\Delta E_m=0.75$ eV agrees relatively well with $\Delta E_m=0.88$ eV published in Ref. 13, which can be related to the properties of a "perfect" crystal lattice. Therefore, the increase of ΔE_m for the second sample implies the presence of crystal defects impeding the diffusion of carbon interstitials C_i.

Because of nearly identical impurity concentrations in the two silicon materials we attribute the different behavior during annealing (annealing rate) to the influence of thermal treatment on the silicon material during the detector fabrication. As can be seen from Table III all samples may be divided into two groups with different heat treatments: a first group of samples with oxide layers of the order of 1000 Å oxidized at temperatures $T_{ox}<1100$ °C (oxidation time $t_{ox}<3$ h) and the other group with oxide layers $d_{ox}>2000$ Å oxidized at $T_{ox}\geqslant1100$ °C (oxidation time up to 20 h). As pointed out in Refs. 7, 14, and 15, high-temperature, long-time oxidations lead to the increase of the oxygen concentration in FZ Si by approximately one order of magnitude.

We assign the higher annealing velocity of the H1 center for detectors with thick oxide layers to a higher oxygen concentration resulting in a higher probability for migrating car-

TABLE II. Silicon material data, oxidation parameters, and investigated defect parameters during room- and low-temperature annealing.

Sample No.	Silicon material	N_D-N_A ($\times10^{10}$ cm^{-3})	N_O[a] ($\times10^{15}$ cm^{-3})	N_C[a] ($\times10^{16}$ cm^{3})	T_{ox} (°C)	t_{ox} (h)	τ ($\times10^4$ s)	ΔE_m (eV)	A ($\times10^{10}$ s^{-1})
BNL 213	Wacker FZ Si 5 kΩ cm	70	3	3	1100	6.0	1.4 ($T=19$ °C)	0.75	0.062
FZR 2-1	FEW FZ Si 1 kΩ cm	300	4	2–6	1000	1.8	2.4 ($T=50$ °C)	1.08	290

[a]The oxygen and carbon concentrations are taken from the silicon manufacturer specification.

TABLE III. High-temperature thermal treatment of the samples during oxidation.

Sample No.	Oxidation temperature T_{ox} (°C)	Atmosphere	Oxide thickness d_{ox} (Å)	Annealing rate
FZR 10-1, 2-1	1000	O_2+3%HCl	1000	slow
FZR A1, A5	900	O_2	1000	slow
PTI A	≥1000	···	≥1000	medium
JINR D4-3-6	1050	O_2+TCA	···	medium
BNL 268-A8	975	O_2	2500	medium
BNL 241-A7	1150	O_2+TCA	9000	fast
BNL 213	1100	O_2+TCA	4500	fast
BNL 253-B7	1200	O_2	9000	fast
PTI G4	1150	O_2+TCA	4000	fast

bon interstitials C_i to meet oxygen interstitials and to form the C_i-O_i complex. This effect was observed also in Ref. 16 using Cz and FZ Si with significant different oxygen concentrations but was not explained by the formation of carbon-related C_i-O_i complexes.

C. H1 and H2 defect transformation

The annealing of the H1 center (interstitial carbon C_i) is accompanied by the concentration increase of the H2 center. A complete understanding of the nature of this defect behavior is still open; however, the H2 center is reported to be a complex of interstitial carbon and oxygen C_i-O_i.[11] The carbon source for this impurity interstitial defect reaction is the H1 center.

The complete radiation induced formation of carbon-related defects in n-type FZ Si is represented as the following:

$$\text{(a)}\quad Si_i + C_s \rightarrow Si_s - (C_i) - \text{defect H1},$$

with subsequent annealing of the interstitial carbon C_i,

$$\text{(b)}\quad C_i + O_i \rightarrow (C_i - O_i) - \text{defect H2}$$

or

$$\text{(c)}\quad C_i + C_s \rightarrow (C_i - C_s) - \text{defect H2}$$

or

$$\text{(d)}\quad C_i + P_s \rightarrow (C_i - P_s) - \text{defect E3}.$$

The DLTS spectra (Fig. 2) and the concentration changes of H1 and H2 (Fig. 4) clearly show that after the complete annealing of the H1 center (approximately after 18 h) the concentration of H2 continues to increase. It is important to note that the room-temperature annealing of the defect H2 for "slow" samples (see Table III) has the same behavior as the "fast" samples. Nevertheless, the values of the relation $H2(t)/H1(0)$ are at least one order of magnitude smaller than the same values for the fast samples during relaxation times up to 280 h. A constant value of $H2(t)/H1(0) \approx 0.4$ has been measured after 5000 h at room temperature and the same constant value was observed after 5 h at an annealing temperature of $T_A = 73$ °C.

Comparing the increase of the H2 center concentration with the concentration decrease of the H1 center we must take into account that it is not possible to determine the

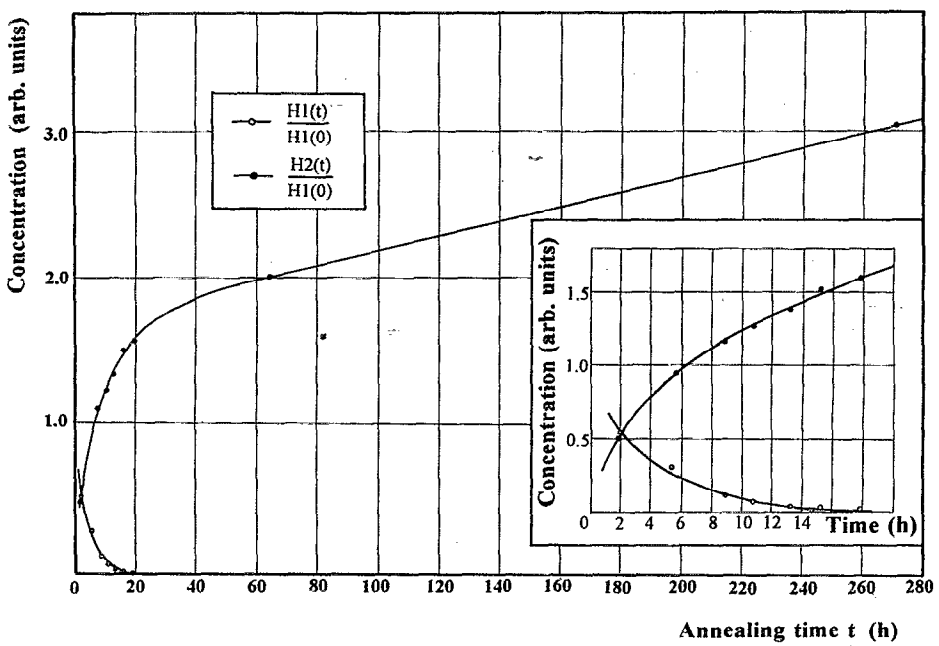

FIG. 4. Concentration changes of the H1 and H2 centers, normalized to the H1 concentration immediately after irradiation (sample no. BNL 213).

absolute concentration from the peaks of the DLTS spectra. This is due to the unknown charge carrier filling factor of the investigated levels after the foreward voltage pulse U_f. This parameter is determined by the electron and hole trapping cross-section ratio, which is $\sigma_n/\sigma_p \leqslant 0.5$ for the H1 and H2 centers. Furthermore, the accuracy of the determination of the H1 and H2 concentrations depends on the stability of the center filling factor after various annealing steps. The error of the determined relative concentrations from the DLTS spectra was $\leqslant 3\%$.

Therefore, concerning the concentration changes of H1 and H2 (Fig. 4) only a qualitative interpretation can be given. The annealing behavior of H1 and H2 suggests that the increase of the H2 concentration is due to two reasons. Actually, there are two components in the kinetics of the H2 concentration change. The duration of the fast component is connected with the annealing time constant of H1 and we conclude that there must be a correlation between the H1 annealing and the formation of the H2 center. The existence of a slow component in the increase of the H2 concentration must be explained by the formation of the C_i-O_i complex arising from another source (not H1) of interstitional C_i with a rather high activation energy and without any level in the band gap. During migration of these carbon interstitials through the crystal additional interstitional carbon atoms C_i are emitted and the reaction (b) continues to go on.

IV. SUMMARY

The behavior of DLTS spectra of radiation-induced defects in high-resistivity FZ-silicon detectors indicates the transformation of carbon-related centers. This transformation of the defects consists of the simultaneous annealing of the interstitial carbon C_i and the concentration increase of the C_i-O_i complexes and occurs at low temperatures (up to 20 °C). The kinetic parameters of the process are affected by the thermal history of the detector, i.e., temperature and duration of the oxidation process. A prolonged and high-temperature oxidation, resulting in the increase of the oxygen concentration in Si, stimulates the fast transformation of C_i centers into C_i-O_i complexes.

The most probable explanation of the astonishing fact that the C_i-O_i complex concentration continues to increase after the exhaustion of the electrically active interstitial carbon implies the existence of neutral carbon interstitials in the crystal. These C atoms can associate with interstitial oxygen forming further C_i-O_i complexes.

[1] E. Fretwurst, N. Claussen, N. Croitoru, G. Lindström, B. Papendick, U. Pein, H. Schatz, T. Schulz, and R. Wunstorf, Nucl. Instrum. Methods A **326**, 357 (1993).
[2] F. Anghinolfi *et al.*, Nucl. Instrum. Methods A **326**, 365 (1993).
[3] E. Barberis *et al.*, Nucl. Instrum. Methods A **326**, 373 (1993).
[4] L. Bischoff, J. von Borany, H. Morgenstern, B. Schmidt, and D. Schubert, ZfK Report, ZfK-579, February 1986.
[5] E. M. Verbitskaya, V. K. Eremin, A. M. Ivanov, and N. B. Strokan, Sov. Phys. Semicond. **27**, 115 (1993).
[6] L. C. Kimmerling, P. Blood, and W. M. Gibson, in *Defects and Radiation Effects in Semiconductors*, edited by J. H. Albany, Inst. of Phys. Conf. Ser. 46 (IOP, Bristol, 1978), p. 273.
[7] B. O. Kolbesen, Solid-State Electron. **25**, 759 (1982).
[8] G. Davies, A. S. Oates, R. C. Newman, R. Woolley, E. C. Lightowlers, M. J. Binns, and J. G. Wilkes, J. Phys. C **19**, 841 (1986).
[9] J. M. Trombetta and G. D. Watkins, Appl. Phys. Lett. **51**, 1103 (1987).
[10] L. W. Song, B. W. Benson, and G. D. Watkins, Appl. Phys. Lett. **51**, 1155 (1987).
[11] M. T. Asom, J. L. Benton, R. Sauer, and L. C. Kimerling, Appl. Phys. Lett. **51**, 256 (1987).
[12] A. R. Bean and R. C. Newman, J. Phys. Chem. Solids **32**, 1211 (1971).
[13] Y. H. Lee, L. J. Cheng, J. D. Gerson, P. M. Mooney, and J. W. Corbett, Solid State Commun. **21**, 109 (1977).
[14] S. D. Brotherton and P. Bradley, J. Appl. Phys. **53**, 5720 (1982).
[15] Zh. Li and H. W. Kraner, Brookhaven National Laboratory Report, NBL-46086, 1991.
[16] L. I. Murin, Phys. Status Solidi A **93**, K147 (1986).